Implementation of a tool for magnetic field mitigation using passive loops

C. A. Wall, *Graduate Student Member, IEEE,* P. L. Arnera, *Senior Member, IEEE,* and M. B. Barbieri, *Senior Member, IEEE.*

***Abstract*—In this paper the implementation of passive loops as a tool for magnetic field mitigation is studied. A theoretical introduction that describes the problem mathematically and physically is presented. Using this formulation a tool to estimate the magnitude and phase of current induced in passive loops is developed and the values obtained are compared with measurements to validate the model. Finally, calculations and measurements are performed for magnetic field with and without the implementation of loops on scale models. The analysis considers different sections of conductors used in loops, and different sizes and shapes.**

***Index Terms*—Magnetic Field, Mitigation, Passive Loops.**

I. NOMENCLATURE

ICNIRP: International Commission on Non-Ionizing Radiation Protection

B: Magnetic flux density [T]

SE: Secretaría de Energía.

II. INTRODUCTION

THE Electric Energy transmission and distribution is associated with Electromagnetic Fields and controversial information have emerged about the possible harmful effects on human health, particularly related to exposure to magnetic fields.

Some enterprises to meet the increasing of electricity demand have been hampered by the manifestation of citizen groups, who oppose the execution of new installations near their homes. This situation is particularly problematic when considering the incorporation of new generation sources in medium and low voltage networks, being necessary to carry to users other electrical system installations.

In 1998, ICNIRP published the Guidelines for Limiting Exposure to Time-Varying Electric, Magnetic, and Electromagnetic Fields, for frequencies up to 300 GHz [1]. The reference levels of magnetic field for the general public were 100 μT and for occupational exposure were 500 μT, at 50 Hz.

In 2002, IEEE published the IEEE StdC95.6-2002 [2], which indicates the IEEE Standard for Safety Levels with Respect to Human Exposure to Electromagnetic Fields, in a frequency range from 0 to 3 kHz. The values of magnetic field limits recommended for the general public were 904 μT, at 50 Hz.

In 2010, ICNIRP published the Guidelines for Limiting Exposure to Time-Varying Electric and Magnetic Fields, with frequencies in the range of 1 Hz to 100 kHz [3]. The reference levels of magnetic field for the general public were 200 μT and occupational level was 1,000 μT, at 50 Hz.

In Argentina, the current regulation was published in 1998 as Resolution SE 77/98 [4]. The maximum levels of magnetic field for the general public is 25 μT, measured at a height of 1 m above ground level, on the edge of the right of way, outside and at the perimeter edge of transformer stations.

Considering the previous concerns, the need to reduce exposure levels to the extent possible arises; there are different techniques to achieve the goal. The passive loops are an effective tool from the technical and economic point of view. This article presents the results obtained in the evaluation of the effect of passive loops for magnetic field mitigation. A standard configuration of low voltage line, with different loops is proposed, for which simulations are performed and are validated by measurements.

III. THEORETICAL FORMULATION AND EXPERIENCES

The magnetic flux density generated by a system of conductors can be estimated by applying the Biot-Savart law, where the conductor current and the geometric arrangement are known.

In this way it is possible to represent the conductors and currents using models and calculation tools. These should be validated by measurements. Next, the procedure used in developing a tool to implement passive loops to mitigate the magnetic field is described.

A. Passive Loops

Compensation by means of passive loops involves to provide a conductor loop in a position such that a voltage is induced as a result of the concatenation of the magnetic flux generated by the phase conductors of a transmission line. As a result of this induced voltage and considering the impedance of the loop, a current flow in this one appears.

This current gives rise to a magnetic field "Bi" which opposes the field generated by the phase conductor current of the line "Br". This situation can be seen in Fig 1.

C. A. Wall, P. L. Arnera and M. B. Barbieri are with IITREE-LAT Facultad de Ingeniería – Universidad Nacional de La Plata, 48 y 116, La Plata (1900), Buenos Aires, Argentina (e-mail: caw@iitree-unlp.org.ar).

978-1-4673-2673-5/12/$31.00©2012 IEEE

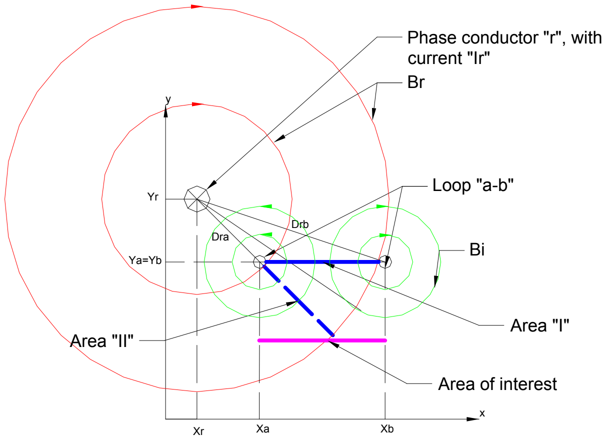

Fig. 1. Magnetic field "B_r" generated by the phase conductor "r", that passes through a passive loop "a-b", which produce a magnetic field "B_i".

B. Induced Current

The calculation of the induced current in a loop must be based on the calculation of the flux that is concatenated in the loop of interest, considering the magnetic field generated by each phase currents. The field generated by the conductor "r" is given by (1) [5][6][7]

$$B_r = \frac{\mu_0 I_r}{2\pi r} \qquad (1)$$

The module of the flux linked with the loop "ab" is given by (2) and the phase angle corresponds to the phase angle of current which produces it: $\theta_{\Phi rab} = \theta_{Ir}$

$$\Phi_{rab} = l\int_{D_{ra}}^{D_{rb}} B_r dr = 2\times 10^{-7} I_r l \ln\frac{D_{ra}}{D_{rb}} \qquad (2)$$

The integration limits come from the concept of *tube of flux*, where the flux through the surface of the loop, Area "I", Fig 1, is the same as that which passes through the Area "II". This calculation is possible because the flux lines are perpendicular to the Area "II".

The module of the induced voltage (U_{rab}) is given by (3) and the phase angle of the voltage (θ_{Urab}) is "-90°" with respect to the flux: $\theta_{Urab} = \theta_{\Phi rab}$ -90°.

$$U_{rab} = \omega \times \Phi_{rab} \qquad (3)$$

Note that the induced voltage depends on the proportion of the flux lines linked.

The inductance of the loop is given by (4)

$$L = \frac{\mu_0}{\pi} l \ln\left(\frac{|X_a - X_b|}{r}\right) \qquad (4)$$

where

l: loop length

r: radius of loop conductor

Loop resistance is given by (5)

$$R = \frac{\rho}{s} l \qquad (5)$$

ρ: conductor resistivity

s: conductor transversal section

The skin effect is neglected for the considered sections.

The modulus of the loop impedance (Z) is given by (6) and the phase angle is given by (7).

$$Z = \sqrt{R^2 + (\omega L)^2} \qquad (6)$$

$$\theta_Z = arctg\frac{\omega L}{R} \qquad (7)$$

Considering (3) and (6), the induced current loop is given by (8).

$$I_{rab} = \frac{U_{rab}}{Z} \qquad (8)$$

The process described here can be applied to a three phase system as in Fig 2, where it is possible to see the three phase conductors and a passive loop in the same level.

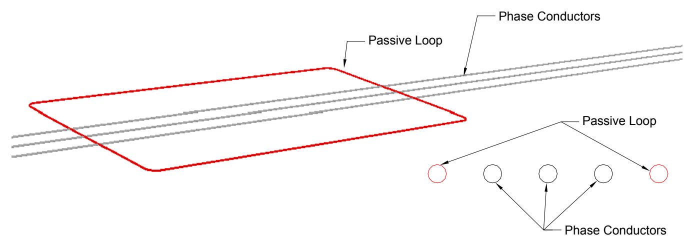

Fig. 2. Three phase conductors and a passive loop in the same level.

If a phasor diagram is plotted, with positive phase reference "R" for the system showed in Fig. 2, Fig. 3 is obtained, where the flux linkage with the coil caused by the phases "R" and "T" and the resulting flux"Φ_{total}" is represented, the central phase flux does not contribute because it is located in the center of the loop. The induced voltage "$U_{induced}$" is situated at "-90°" from "Φ_{total}" and backward with respect to this, the induced current "$I_{induced}$" comes.

This methodology was used to calculate the induced currents in loops for different cases presented in Table I, where features of the used loops are shown. For all cases a frequency of 50 Hz was considered.

The separation between the phase conductors was 0.25 m in all the considered cases. The case "0" corresponds to the implementation of the line without the presence of passive loops.

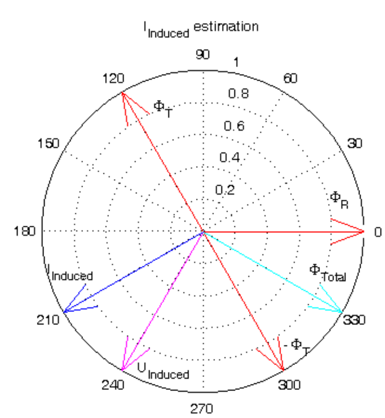

Fig. 3. Induced current, phasor diagram with Φ_{total}, I_{ind} y U_{ind}.

TABLE I
CASES CONSIDERED

Case	Loop Section	Loop Width	Loop Length	Secuence
	[mm^2]	[m]	[m]	
1	35	1,0	2,85	RST
2	35	1,0	2,85	RTS
3	95	1,0	4,45	RST
4	95	1,0	4,45	RTS
5	95	1,5	4,00	RST
6	95	0,5	4,75	RST

C. Induced Current Measuremet

In order to verify the proposed mathematical physical model, an experimental model was carried out, and different loop configurations were implemented, considering different sections of conductors and loop areas. In Fig. 4 an experimental setup used for testing is presented. This shows the phase conductors and one of the loops installed. In all cases horizontally coplanar configuration was considered.

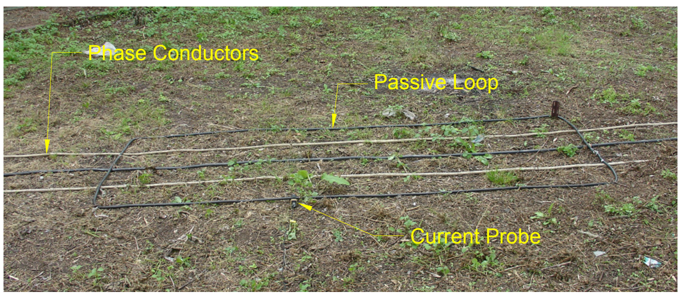

Fig. 4. Experimental circuit, phase conductors, passive loop and measuring element.

For current injection a current source was used with four channels of 30 A and 200 VA each. It is possible to adjust the magnitude and phase of each channel.

For induced current measurement in the loop a current clamp was used whose maximum range is 5 A, accuracy 1% between 1 and 5 A, and phase shift 4 ° between 100 mA and 5 A. A current clamp with 30 A in range was used to measure the reference phase current, its accuracy and phase angle error are 5 % and 5 °, respectively. Both measured currents were applying in a four-channel oscilloscope, 100 MHz and 1 GS / s.

Amplitude and phase difference currents were recorded and measured for each case. The angle of phase current "R" was used as a reference (defined as 0º). Fig. 5 shows one of the records obtained, it shows the reference phase current, the current induced in the loop and the waveform that represents the calculated current for the case 1. The currents induced in the loop were enlarged in order to appreciate it.

Table II presents the results of the Measured (M) and Calculated (C) currents in cases 1 to 6.

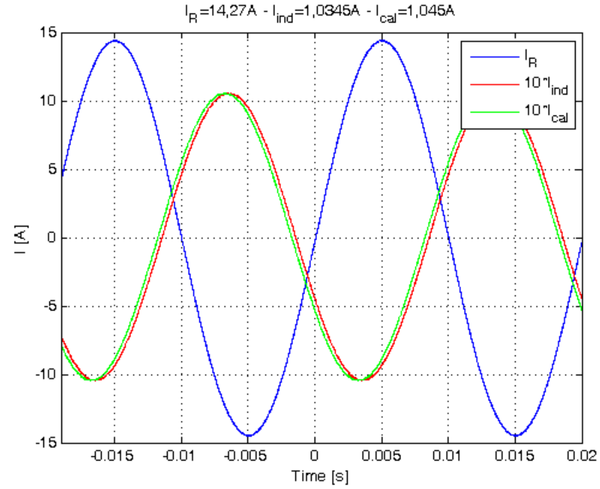

Fig. 5. Phase currents and loop current, calculated and measured for sequence RST.

TABLE II
COMPARISON OF MEASURED AND CALCULATED VALUES OF INDUCED CURRENT

Case	I_{phase}	$I_{Loop.\,C}$ Mod.	$I_{Loop.\,C}$ Phase	$I_{Loop\,M}$ Mod.	$I_{Loop\,M}$ Phase
	[A]	[A]	[°]	[A]	[°]
1	14,3	1,05	-147	1,03	-135
2	14,3	1,05	-86	1,04	-90
3	14,9	1,98	-166	1,9	-175
4	14,9	1,98	-107	1,9	-116
5	14,8	1,1	-167	1,04	-175
6	14,9	1,1	-106	1,06	-114

D. Passive Loop Impedance Analysis

Table III presents the results of the calculated values for the impedance considered in each case. Case "0" considers the circuit without passive loops.

TABLE III
CALCULATED VALUES OF IMPEDANCE AT 50 HZ

Case	Loop Section	Loop Width	Loop Length	R	L	X	Z
	[mm^2]	[m]	[m]	[mΩ]	[μHy]	[mΩ]	[mΩ]
1	35	1,0	2,85	5,8	10,1	3,2	6,6
2	35	1,0	2,85	5,8	10,1	3,2	6,6
3	95	1,0	4,45	2,75	9,3	2,92	4,01
4	95	1,0	4,45	2,75	9,3	2,92	4,01
5	95	1,5	4,00	2,75	9,02	2,83	3,95
6	95	0,5	4,75	2,75	8,6	2,7	3,86

E. Magnetic Field Calculation and Measurement

Once the value of the induced current in the loop is calculated, it is possible to calculate the resulting field "B_0" according to (9).

$$\overrightarrow{B_0} = \overrightarrow{B_r} - \overrightarrow{B_i} \qquad (9)$$

The measurement procedures of magnetic fields produced by lines and facilities of power frequency are described in IEEE 644-1994 [8] and IEC 61786:1998 [9] standards. They suggest two ways to quantify the fields, one for a single axis probe (single coil) and one for three-axis probe's, with three orthogonal coils. In both cases it is assumed that the variation of the field components are sinusoidal.

According to the standards, the indication of a three-axis meter, called resultant magnetic field (B_R), is given by the expression (10).

$$B_R = \sqrt{B_X^2 + B_Y^2 + B_Z^2} \qquad (10)$$

Where B_X, B_Y and B_Z are the rms values of the three orthogonal field components.

For magnetic field measurements a three-axis magnetic field meter, with an accuracy of 8%, was used.

The magnetic field calculations were carried out with three-dimensional models and the magnetic fields values on each axis was calculated, the B_R was obtained according to (10). The results are presented by means lateral profiles with results of measurement and simulations.

F. *Magnetic Field Results*

This section shows the results for the calculations (C) and measurements (M) of magnetic fields in the experimental cases presented above. They were carried out by means lateral profiles of the line considered.

The values obtained from simulations are shown in full plot. The points represent the results of measurements. For each case the same colors are used in calculations and measurements.

The background magnetic field was measured before energizing the circuit, with no current in the phase conductors.

Figs. 6 and 7 show the results obtained for cases 1 to 4.

The differences between Figs. 6 and 7 cover two aspects: different section of the conductor section and different loop area.

Best results were obtained in the case of greater loop area and a larger section of conductors.

Figure 8 shows the results obtained for the same section of conductor, 90 mm^2, but considering different loop geometries.

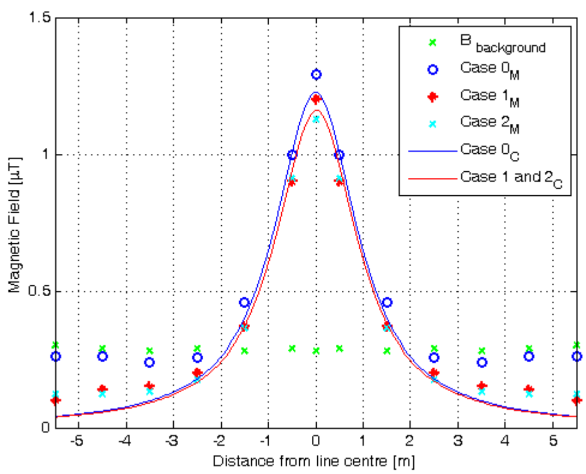

Fig. 6. Lateral Profiles obtained for cases 1 and 2, with I = 14.9 A, measured and calculated values.

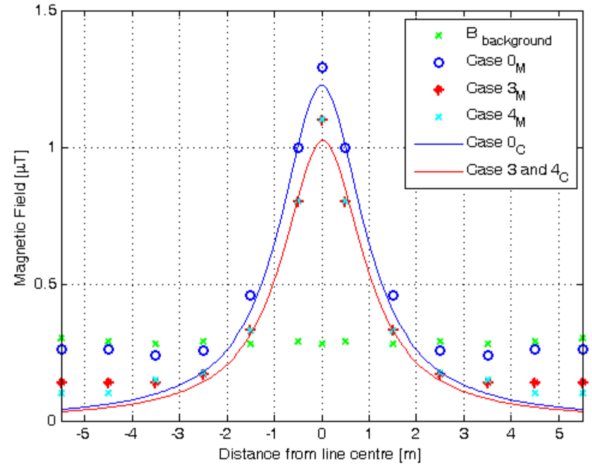

Fig. 7. Lateral Profiles obtained for cases 3 and 4, with I = 14.9 A, measured and calculated values.

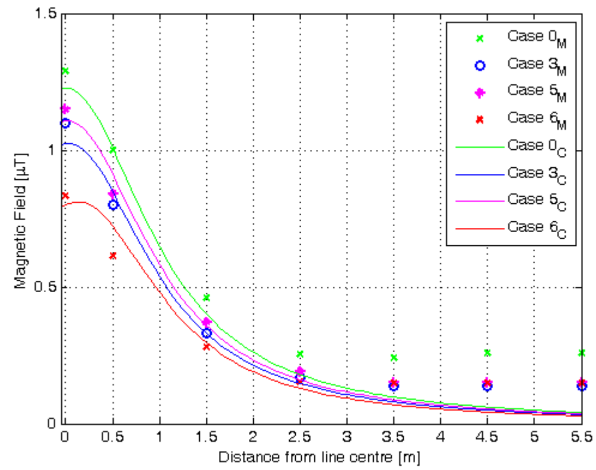

Fig. 8. Profiles obtained for cases 0, 3, 5 and 6, with I = 14.9 A, measured and calculated values. Conductor loop cross section: 90 mm^2.

G. *Results Analysis*

Regarding to the loop induced currents, it can be concluded that when larger cross section conductors are considered, the resistance is lower and a decrease in loop impedance is obtained.

If the geometry of the loop is changed with no changes in the section and length of the conductor, and the width and length of the loop change, it is possible to see that the inductive reactance is modified, and consequently changes in the impedance are observed. But this is not necessarily reflected as an increase of the induced current, because a configuration can yield higher impedance, but the concatenated flux lines are greater and the induced voltage can be increased.

It should be noted that when measurements are taken it is possible to have influence of external sources of power frequency magnetic field in the surrounding. This can be seen in all presented cases. During the implementation of the described circuits the existing level was measured without energizing the installation and it was found that some of these values can be important in certain areas.

Calculated values were verified by means measurements of different geometric alternatives and this was checked exciting the circuit for different phase sequences.

Figure 9 shows the phasor diagrams representing the calculated and measured values for sequences RST (D) and RTS (I), using a 35 mm^2 conductor. The values of the loop induced currents were multiplied by 10 to see the module.

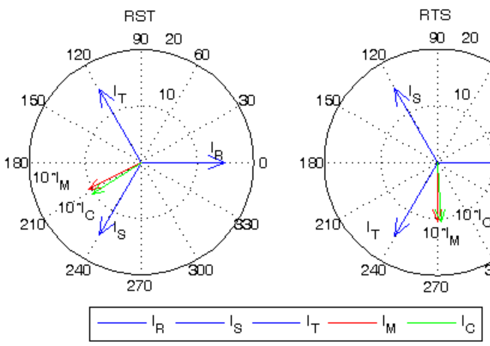

Fig. 9. Phase currents and current loop, calculated and measured for RST and RTS sequence using 35 mm^2 conductors.

Respect to the magnetic field, the differences between the measured and calculated values are within the measurement instrument error, in all cases they are below 6%.

Furthermore, as the measurements deviate from the axis of the system, it is showed that greater differences exist with the previously indicated, this is because in such area exists influence of external sources of magnetic field that are not covered by the calculations. This can be verified with measurements made without current.

IV. Conclusions

A study of magnetic field mitigation was carried out by means of passive loops. The overall aim was to implement the use of loops and developed calculation tools that enable to know the behavior of different geometrical characteristics of the loops.

The proposed model was validated by measurements. The differences found in all cases were within the errors of the used instruments. Regarding to the modules of the induced currents, there are substantially equal, whereas the phase difference falls within the error of the instruments used.

In reference to the magnetic field, the calculation tool used shows similar results to the measurement (within the instrument error) in the area near the center of the line. As the field B is evaluated at points away from this area is bigger differences, which are due to external magnetic field, not included in the models.

In the calculations it was not taken into account the influence of the earth conductivity, all cases were implemented on the surface of the earth and there was no influence of this on the measured values in reference to those calculated.

It is considered that the developed tool accomplishes the goal of providing acceptable results when implementing passive loops to mitigate the magnetic field and predict their behavior in certain areas of interest.

It is intended to use this tool to mitigate the magnetic field in systems with different geometrical characteristics.

V. References

[1] "Guidelines for Limiting Exposure to Time-Varying Electric, Magnetic, and Electromagnetic Fields (up to 300 GHz)". ICNIRP 1998. Health Physics 74(4), 494-522.

[2] IEEE StdC95.6-2002: IEEE Standard for Safety Levels with Respect to Human Exposure to Electromagnetic Fields, 0-3 kHz.

[3] "Guidelines for Limiting Exposure to Time-Varying Electric and Magnetic Fields (1 Hz to 100 KHz)". ICNIRP 2010. Health Physics Society 15 June 2010, 818-836.

[4] Resolución SE 77/98, Secretaría de Energía de la Nación (Argentina). Boletín Oficial N° 28.859 1ª Sección

[5] A. V. Netushil, K. M. Polivanov, *Principios de Electrotecnia 3*, vol. III. Grupo Editor de Buenos Aires, 1980.

[6] K. Yamazaki, T. Kawamoto and H. Fujinami, "Requirements for Power Line Magnetic Field Mitigation Using a Passive Loop Conductor" *IEEE Trans.on Power Delivery*, vol. 15, No. 2, pp. 646-651, April 2000.

[7] CIGRÉ TB 373 "Mitigation Techniques of Power-Frequency Magnetic Fields Originated From Electric Power Systems", WG C4.204, February 2009

[8] IEEE Std 644™-1994 (R2008), "IEEE Standard Procedures for Measurement of Power Frequency Electric and Magnetic Fields From AC Power Lines"

[9] IEC61786:1998, "Measurement of low-frequency magnetic and electric fields with regard to exposure of human beings-Special requirements for instruments and guidance for measurements"

VI. Biographies

PatriciaLiliana Arnera was born in Buenos Aires, Argentina, on April 27, 1958. She got her degree in Electrical Engineering from the UNLP in 1981. Her special field of interest includes Electrical Power Systems. She works for the IITREE-FI-UNLP studying transient conditions of electrical systems and working in Electromagnetic Fields and health. As a researcher of the IITREE she has made technical works for public and private companies of electrical service and industry in Argentina. She is Full Professor of Power System at the EE Dept., School of Engineering, UNLP. She has been IITREE director since 1998. She was Argentina PES Chapter Chairman in 2001-2002.

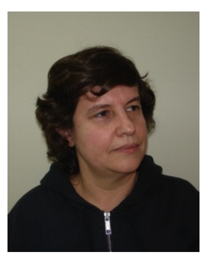

M. Beatriz Barbieri was born in Laprida, Argentina, on July 5, 1960. She got her degree in Telecommunications Engineering (with honors) from UNLP in 1984. Her special field of interest includes Electrical Power Systems. She has been working for the IITREE-FI-UNLP studying normal and transient conditions of electrical systems and in economic and technical planning since 1983. As a researcher of the IITREE she has made technical works for public and private companies of electrical service and industry in Argentina. She is Professor of Electricity and Magnetism at the EE Dept., School of Engineering, UNLP. She is IEEE member of Power Electric Society.

Carlos A. Wallwas born in Posadas, Argentina, on February 7, 1979. He got his degree in Electrical Engineering from the UNLP in 2006. Since her graduation, he works in the IITREE-FI-UNLP, his special field of interest includes Electromagnetic Fields and Health, and Electric Systems Environmental Performance. He is Assistant of Electricity and Magnetism at the EE Dept., School of Engineering, UNLP. He has made a lot of technical works for public and private companies of electrical service and industry in Argentina. He is IEEE member of Power Electric Society. He is member of the National Argentinean CIGRE SC C3 "System Environmental Performance".